Whole-body somatotopic maps in the cerebellum revealed with 7T fMRI

Boillat, Y.; Bazin, P.-L.; van der Zwaag, W.

DOI
10.1016/j.neuroimage.2020.116624

Publication date
2020

Document Version
Final published version

Published in
NeuroImage

NeuroImage 211 (2020) 116624

Contents lists available at ScienceDirect

NeuroImage

journal homepage: www.elsevier.com/locate/neuroimage

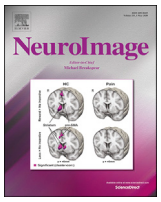

Whole-body somatotopic maps in the cerebellum revealed with 7T fMRI

Yohan Boillat [a], Pierre-Louis Bazin [b,c], Wietske van der Zwaag [d,e,*]

[a] Laboratory for Functional and Metabolic Imaging, Ecole Polytechnique Fédérale de Lausanne, Lausanne, Switzerland
[b] Integrative Model-Based Cognitive Neuroscience Research Unit, University of Amsterdam, Amsterdam, the Netherlands
[c] Departments of Neurology and Neurophysics, Max Planck Institute for Human Cognitive and Brain Sciences, Leipzig, Germany
[d] Animal Imaging and Technology Core (AIT), Center for Biomedical Imaging (CIBM), Ecole Polytechnique Fédérale de Lausanne, Lausanne, Switzerland
[e] Spinoza Centre for Neuroimaging, Amsterdam, the Netherlands

ARTICLE INFO

Keywords:
Cerebellum
Somatotopy
Somatosensory
Motor
fMRI
High spatial resolution

ABSTRACT

The cerebellum is known to contain a double somatotopic body representation. While the anterior lobe body map has shown a robust somatotopic organization in previous fMRI studies, the representations in the posterior lobe have been more difficult to observe and are less precisely characterized. In this study, participants went through a simple motor task asking them to move either the eyes (left-right guided saccades), tongue (left-right movement), thumbs, little fingers or toes (flexion). Using high spatial resolution fMRI data acquired at ultra-high field (7T), with special care taken to obtain sufficient B_1 over the entire cerebellum and a cerebellar surface reconstruction facilitating visual inspection of the results, we were able to precisely map the somatotopic representations of these five distal body parts on both subject- and group-specific cerebellar surfaces. The anterior lobe (including lobule VI) showed a consistent and robust somatotopic gradient. Although less robust, the presence of such a gradient in the posterior lobe, from Crus II to lobule VIIIb, was also observed. Additionally, the eyes were also strongly represented in Crus I and the oculomotor vermis. Overall, crosstalk between the different body part representations was negligible. Taken together, these results show that multiple representations of distal body parts are present in the cerebellum, across many lobules, and they are organized in an orderly manner.

1. Introduction

The cerebellum has a significant role in sensory-motor control, and shows a distinct somatotopic organisation, similar to the organisation found in the motor and sensory areas of the cerebral cortex. In contrast to the forebrain sensorimotor regions, cerebellar responses are found ipsilateral to the stimulated body part, consistent with the double decussation of the majority of afferent and efferent pathways where a first crossing to the other side of the body of the ventral spinocerebellar tract occurs in the spinal cord, followed by a second crossing at the level of the cerebellum. Early studies using afferent electrical stimulations in cats and monkeys observed a somatotopic pattern located in the anterior lobe (Adrian, 1943). It was later shown that such responses were also observed in the posterior lobe (lobule VIII) of the cat (Snider and Stowell, 1944). The development of functional magnetic resonance imaging (fMRI) further confirmed such an organization in humans (Batson et al., 2015; Nitschke et al., 2007; Grodd et al., 2001; van der Zwaag et al., 2013; Wiestler et al., 2011). Several particularities pertain to the cerebellum, such as the multiple representations of a specific body part. For instance, the hand digits are represented in both lobule V and VIII with a somatotopic organization, but also in Crus I, though there not with a specific pattern (van der Zwaag et al., 2013). Another particularity, observed at the sub-millimeter scale in rodents using electrophysiological recordings, is the so-called fractured somatotopy where the body map is broken up into smaller representations similar to a mosaic (Shambes et al., 1978). However, such an organization was never observed in humans due to the limited spatial resolution of non-invasive methods. In humans, fMRI results obtained in the hemispheric anterior lobe, combined with lobule VI, tend to show an anterior to posterior organization (lobule II to lobule VI) going from the feet representations via the hands to the head (Grodd et al., 2001; Rijntjes et al., 1999; Schlerf et al., 2010). Although several body parts were also shown to be represented in the posterior lobe, the pattern seems to be more variable across participants and studies, and often no clear somatotopic organization was observed (Batson et al., 2015; van der Zwaag et al., 2013; Wiestler et al., 2011). However, Grodd et al. (2001) suggested such an organization in the posterior lobe did exist, although the number of body part representations was not large enough to infer about the presence of a gradient.

* Corresponding author. Mijbergdreef 75, 1105BK Amsterdam, the Netherlands.
E-mail address: w.vanderzwaag@spinozacentre.nl (W. van der Zwaag).

https://doi.org/10.1016/j.neuroimage.2020.116624
Received 4 October 2019; Received in revised form 20 December 2019; Accepted 6 February 2020
Available online 11 February 2020

Further evidence was then obtained using functional connectivity analysis with seeds in the primary motor cortex demonstrating a cerebellar foot-hand-tongue organization (Buckner et al., 2011) or task activation maps from a very large dataset (Guell et al., 2018a). Results regarding the cerebellar somatotopic organization are still sparse compared to the motor and sensory cortices, especially concerning the posterior lobe. One of the reasons may be due to the potential fractured somatotopy, which cannot be resolved using fMRI, leading to overlap across body parts and between-subject variability as peak activations might not overlap. Moreover, the cerebellum remains a challenging part to image compared to the cerebrum as it often suffers from a low B_1 transmit field (Vaidya et al., 2018) and physiological noise contamination (van der Zwaag et al., 2015) especially impacting the posterior lobe. Additionally, the fine cerebellar structure requires high spatial resolution data for a proper grey/white matter (GM and WM, respectively) segmentation and precise functional mapping. Such data can be provided using ultra-high field MRI, where a precise delineation of the *arbor vitae* can be obtained in a reasonable amount of time (Marques et al., 2012, 2010b). Taking advantage of 7 T MRI, we acquired high spatial resolution functional and structural data in order to investigate the fine somatotopic organization of five different body parts (i.e. toes, little fingers, thumbs, tongue and eyes) of the cerebellum at both subject and group levels. By using a dedicated processing pipeline for high spatial resolution cerebellar data analysis (Boillat et al., 2018), we were able to obtain group-specific cerebellar surfaces minimizing between-subject variability and enabling accurate mapping of somatotopic representations in the whole cerebellum.

2. Methods

2.1. Participants

Nine healthy participants (5 females, 18–27 years old) were recruited to participate in this study. All participants were right-handed and had good or lens-corrected vision. They all provided written informed consent prior to participation and this study was approved by the local ethics committee. Federal and Local guidelines were followed throughout the study.

2.2. MR acquisition

All participants were scanned on a head-only 7-T/68 cm MRI scanner (Siemens Medical Solutions, Germany) using a 32-channel head coil (Nova Medical USA). Functional data were acquired with a sinusoidal EPI sequence (repetition time TR = 2700 ms, echo time TE = 28 ms, phase-encoding acceleration factor = 2, matrix 154 × 154 × 46, voxel size 1 × 1x1 mm^3, coronal-oblique acquisition). Six functional runs of 281s each (104 images) were executed. A whole brain T_1 image was obtained using the MP2RAGE sequence (Marques et al., 2010a) including fat navigators (Gallichan et al., 2015) with TR = 6000 ms, TE = 2.05, first inversion time TI_1 = 800 ms, second inversion time TI_2 = 2700 ms, first excitation flip angle = 7°, second excitation flip angle = 5°, matrix 320 × 256 × 320, voxel size 0.6 × 0.6 × 0.6 mm^3. A B_1 map was acquired with a SA2RAGE sequence (Eggenschwiler et al., 2012; TR = 2400, TE = 0.79, matrix 128 × 128 × 64, voxel size 2.0 × 2.0 × 2.5 mm^3). The SA2RAGE was acquired with the same transmit voltage as the MP2RAGE. Respiratory and cardiac traces were recorded with external sensors during the functional runs. To improve the inversion efficiency over the cerebellum and whole brain B_1 homogeneity, two dielectric pads were placed around the upper neck during the whole session (Teeuwisse et al., 2012; Vaidya et al., 2018).

2.3. Paradigm

The participants were asked to perform a motor task following a visual cue indicating which body part to move. Five different body parts were targeted: bilateral toes (all ten), bilateral thumbs, bilateral little fingers (LF), tongue and eyes. Each trial started by the display of which body part to move (1s) followed by a small dot flickering at 1Hz indicating the movement pace. Each trial lasted 15s followed by a resting period of 10s with a displayed fixation cross as control condition during which the participants were asked to stay still. For the toes and fingers, the movement was performed in a flexion-extension manner. The tongue was moved left-right while touching the teeth. For the eyes, the dot alternatively jumped to the right and left sides of the screen and the participants had to visually follow it, requiring them to make a horizontal saccade. The participants were instructed to isolate the movements as much as possible. No other restraining method was applied. Each body part was tested twice per run for a total of 12 trials in six runs. The body part order was randomized for each run.

2.3.1. Structural data processing

Subject-specific surfaces of the cerebellum were created based on the T_1-maps which were then averaged across participants. First, the T_1-maps were corrected for residual B_1-inhomogeneities using the SA2RAGE B_1-map (Marques and Gruetter, 2013). The skull-stripping step was performed using BET (part of FSL package; Smith, 2002). All further processing of the T_1-maps was done using the CBS Tools toolbox (Bazin et al., 2013; https://github.com/piloubazin/cbstools-public/) following the exact same procedure as in (Boillat et al., 2018). Namely, the T_1-maps, which were thresholded at 4000 ms, were brought into the MNI space using a global linear registration algorithm based on FLIRT (Jenkinson and Smith, 2001). Then they were segmented into cerebellum white (WM) and (GM) matter, which are among the 30 structures segmented using the multi-geometric deformable model (MGDM) segmentation algorithm (Bogovic et al., 2013). In addition to the T_1-maps, filters for dura matter, cerebrospinal fluid (CSF) and arteries were added as inputs to the MGDM algorithm (Bazin et al., 2014). A cerebellar mask, which was manually corrected to remove extra-cerebellar tissues, such as remaining small parts of the occipital cortex and brainstem that were not properly segmented with the MGDM algorithm, was created from the merging of WM and GM. The masked T_1-maps were then segmented using the Fuzzy and Noise Tolerant Adaptive Segmentation Method (FANTASM; Pham, 2001) providing a precise delineation of GM, WM and cerebrospinal fluid (CSF) borders. FANTASM is an unsupervised clustering algorithm based on image intensities, and robust to noise and inhomogeneity. The WM-GM border and GM-CSF border level sets were then extracted with an adaptation of the cortical reconstruction using implicit surface evolution algorithm (CRUISE; Han et al., 2004). CRUISE is a topology-preserving technique which ensures spherical topology. Using the level sets, a continuous layering of the cerebellar cortex was built at three different cortical depths following a volume-preserving model of cortical folding (Waehnert et al., 2014) with each layer representing one third of the total cortical thickness. The inner, middle and outer surfaces where realigned using a diffeomorphic image registration algorithm (ANTs; Avants et al., 2008) to a high-resolution template (CHROMA atlas, a group-wise average of a T_1-map acquired at 0.7 mm isotropic resolution) from the CBS Tools. The aligned level set representations of the surfaces are then averaged across subjects for each separate surface and the final group average surface is extracted as their zero-level set.

From this, three types of cerebellar surfaces were obtained: i) subject-specific surfaces in the MNI space, ii) averaged surfaces across participants in the space of the CHROMA atlas and iii) an inflated surface generated from the CHROMA atlas.

2.4. Functional data processing

The functional EPI data was processed with SPM12 (http://www.fil.ion.ucl. ac.uk/spm) and home-built Matlab scripts (R2014a, The MathWorks, Inc. USA). The EPI data were slice-timing corrected, realigned and smoothed (1.5 × 1.5 × 1.5 mm^3 FWHM). A first level general linear model (GLM) was created with one regressor per body part convolved

with the canonical hemodynamic function, 10 physiological traces as nuisance regressors obtained from RETROICOR (Glover et al., 2000) and 6 motion regressors, for a length of 104 data points per regressor time series per run. The six runs per participants were included as independent sessions in the same SPM design matrix. The contrast images (con_*, weighted combination of the beta images) resulting from this analysis were then normalized into the CHROMA space in order to perform a second level analysis using a nonparametric permutation method (SnPM, cluster-forming threshold CDT = 0.001, $p < .05$ corrected for family-wise error (FWE) at cluster-level, http://warwick.ac.uk/snpm). Label maps were created at both subject- and group-level representing the five body parts by using the results of the F-tests as a mask for which each voxel was labelled as the body part showing the highest T value (also see Martuzzi et al. (2014)). In order to investigate how much these labels were specific to their corresponding body parts, each label was used as a region of interest (ROI) to extract the T-values across the five body parts.

Additionally, overlap maps depicting the number of times a voxel was labelled as a specific body part for all participants were created and mapped on the inflated cerebellar surface. Finally, the centre of gravities (COG) for each body part and participant were computed. To do so, the cerebellum was subdivided into four different regions: left and right anterior lobes (including lobules I, II, III, IV, V and VI) and left and right posterior lobes (including lobules VIIb, VIIIa, VIIIb, IX and X). Note that although lobule VI is usually attributed to the posterior lobe, it shares somatotopic maps coming from the anterior lobe (Fig. 4). Crus I and Crus II were not taken into account for the COG as the inspection of subject- and group-specific surfaces did not reveal any consistent somatotopic organization in these regions. To compute the COG, T maps of each body part were used where only the highest fifty T values, equivalent to a volume of 6.25 mm^3 (T maps are resliced according to the CHROMA atlas resolution), were taken into account for the computation. This number of voxels was chosen as it still represents a small volume and, therefore, preserves the advantage of our high resolution data, while being less sensitive to aberrant high values due to noise. The Euclidean distances between the COGs were computed for the four regions. In order to confirm the presence of a somatotopic gradient, a similar approached as in Akselrod et al. (2017) was used: A principal component analysis (PCA) was performed for the four COG sets to determine the new axis explaining the most variance (first principal component; PC) in the CHROMA space. The ordering of the different body parts based on the coordinates along the first PC was statistically tested using a Page test (Page, 1963). The hypothesis that the gradient was organized in the order eyes – tongue – thumbs – little fingers – toes, as based on previous reports (Batson et al., 2015; Grodd et al., 2001; van der Zwaag et al., 2013), was

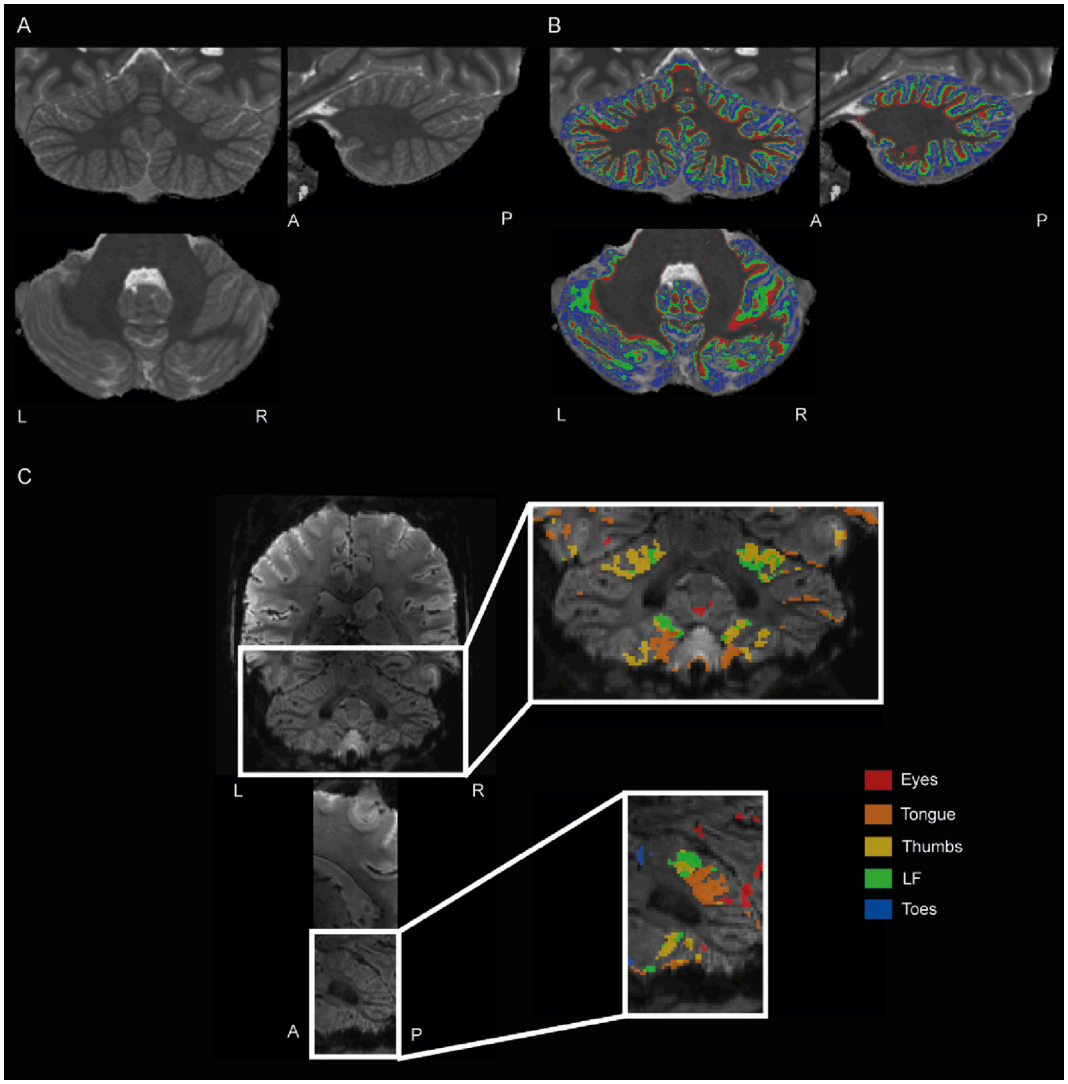

Fig. 1. A) T_1 image acquired at 0.6 mm isotropic resolution providing sufficient resolution to delineate the different folia and arbor vitae. B) Layering of the cerebellar grey matter at three different cortical depths: inner (red), middle (green) and outer (blue). C) Functional EPI image of 1 mm resolution with the somatotopic label map of a single subject. L/R stands for left/right orientations and A/P for anterior/posterior orientations.

tested. The test provided an L-statistic, which is the equivalent of an F value for an F-test. Additionally, the statistical results of 1000 random permutations were also reported. Values for statistical significance were obtained from Page (1963). The custom Matlab and CBS Tools scripts used in this study can be found at https://github.com/yboillat/Cerebellum_somatotopy. The single-subject T maps in native space can be found at https://identifiers.org/neurovault.image:317112.

3. Results

3.1. Brain segmentation and surface generation

The high resolutions of the T_1 maps and sufficient B_1 field resulted in a good segmentation of the cerebellum with a clear delineation of the GM/WM border in the different lobules (Fig. 1A and B). The subject-specific surfaces also clearly show the fine cerebellar structure, especially for the anterior lobe (Fig. 2). However, the segmentation of the posterior lobe was sometimes underestimated, likely due to lower SNR associated with B_1+ field inhomogeneities in this region (Fig. S1).

3.2. Single-subject functional results

The functional EPI data was acquired at sufficient resolution to enable the observation of most of the arbor vitae (Fig. 1C). Regarding the functional activity, all participants showed functional activity based on the F-test ($p < .001$ uncorrected) including the five body parts in both the

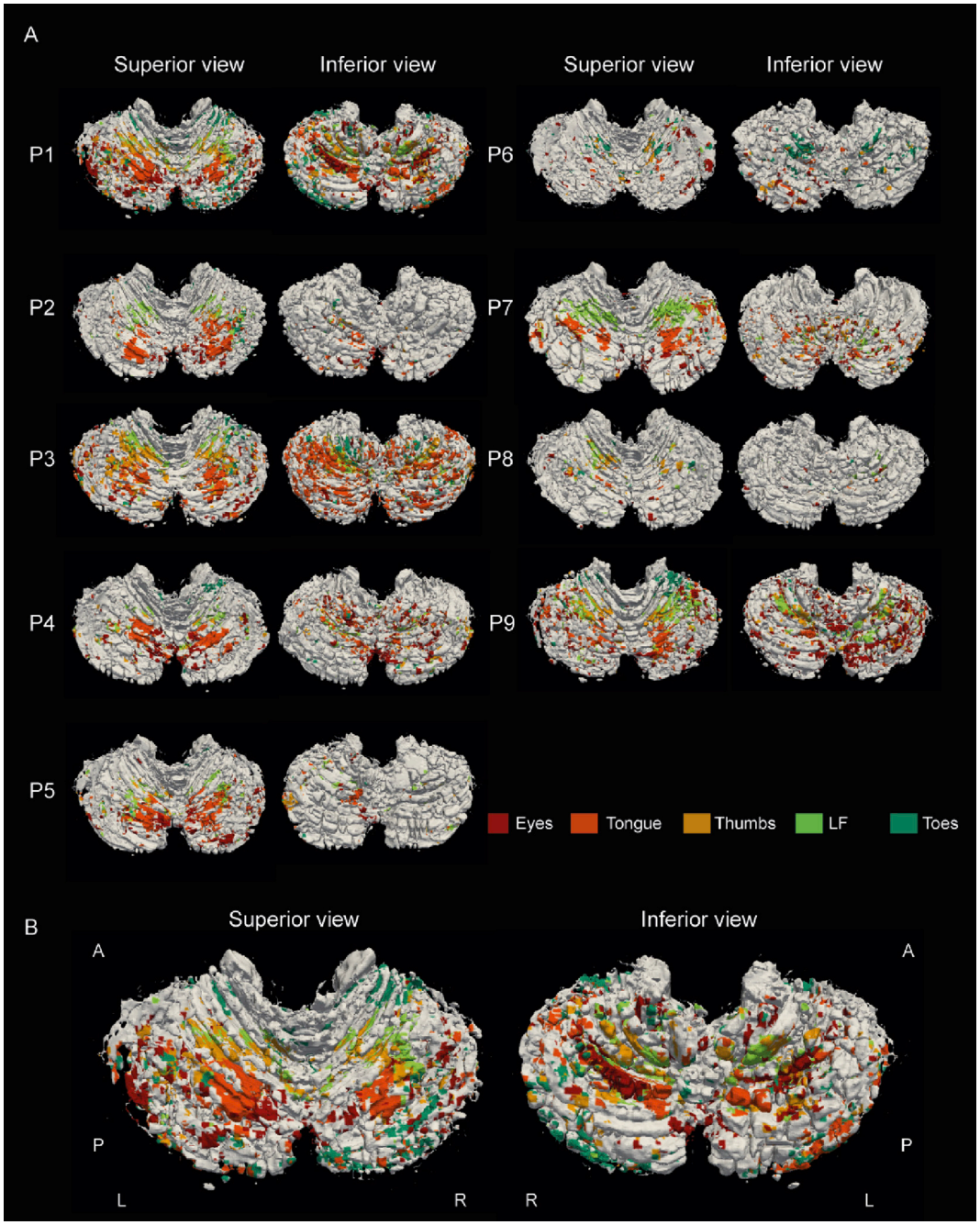

Fig. 2. A) Subject-specific cerebellar surfaces (top and bottom views) of the nine participants on which the somatotopic labels are mapped. The label maps were generated by using the F-test results ($p < .001$ uncorrected) as a mask where each voxel was attributed to the body part showing the highest T-value. B) Enlarged surface of participant P1. L/R stands for left/right orientations and A/P for anterior/posterior orientations.

anterior and posterior lobes (Fig. 2). Participants generally showed large activation clusters with an averaged F-test cluster size of $1 \times 10^5 \pm 0.6 \times 10^5$ voxels (mean ± standard deviation) across participants, except for P2, P6 and P8 (0.4×10^5, 0.4×10^5 and 0.2×10^5 voxels, respectively) who showed substantially smaller clusters. The tongue, thumbs and little fingers are the most consistently observed activity patches at single subject-level, while the toes and eyes representations seem to be more variable. When following the eyes – tongue - thumbs – little fingers – toes organization, a gradient can be observed following a medial-posterior to lateral-anterior orientation.

The labels are found to be selective for their corresponding body part. Crosstalk was absent between toes, tongue, fingers and eyes. Only the stimulation of little fingers and thumbs elicited small BOLD responses in the other digits ROI (Fig. 3). This shows that the different body part representations do not significantly overlap.

3.3. Group level functional results

The averaged surface on which the group labels are mapped clearly shows the somatotopic gradient observed at the single-subject level on the anterior lobe (Fig. 4), where the eyes are represented in the medial-posterior area followed by the tongue, thumbs, little fingers and finally the toes when moving along the gradient in the lateral-anterior direction (lobule VI to lobule I). The tongue and finger representations show the largest areas with the thumbs and little fingers clusters being entangled. As observed in the single-subject level results, the posterior lobe shows a less robust somatotopic organization with a large area taken up by the tongue representation. However, a pattern is still observable with a posterior to anterior gradient, close to the vermis. This is confirmed when looking at the number of label overlaps for each body parts (Fig. 5 bottom view), where the eyes are located close to the vermis (lobule VI) with the gradient finishing in lobule IV. Additionally, a significant part of the eyes representation is located in the vermis and Crus I area. Note that in the label overlaps maps the somatotopic gradient can be seen in both the left and right cerebellar hemispheres. A schematic representation of the obtained somatotopy is given in Fig. 7.

3.4. Distances and organisation of COG

The COGs show a clear somatotopic organization in both anterior lobes (Fig. 6A). A gradient can be observed in the three different planes (axial, coronal and sagittal) along the first PC. A similar pattern is found for the left posterior lobe. In contrast, the right posterior lobe showed more variability in its organization with individual COG being less grouped per body part. However, the eyes – tongue – thumbs – little fingers – toes somatotopic order, as computed by the Page test, was significant for all the four tested regions (Table 1).

The average distances between the different body parts is consistent with the presence of a somatotopic gradient (Fig. 6B). The close organization of the thumbs and little fingers can also be observed.

4. Discussion

The present study aimed to show the somatotopic organization of the main distal body parts in the entire cerebellum. By using a simple motor task including toes, little fingers, thumbs, tongue and eyes, we were able to obtain cerebellar motor-related activity across all participants. Additionally, the quality and resolution of anatomical T_1 maps were sufficient enough to provide single-subject surfaces allowing a precise somatotopic mapping. The anterior lobe (including lobule VI) showed the most robust somatotopic organization, consistently observed at both subject- and group-level. Extending the earlier findings of previous fMRI studies (Buckner et al., 2011; Nitschke et al., 2007; Grodd et al., 2001; Guell et al., 2018a; van der Zwaag et al., 2013), we found the bilateral eyes-to-toes gradients follows a medio-posterior to latero-anterior orientation, passing through lobules IV to VI, contrasting with early reports of a central homunculus (Snider and Eldred, 1951; Snider and Stowell, 1944).

Interestingly, we observed a similar somatotopic gradient in the posterior lobe were the five body parts are represented from Crus II to lobule VIIIb (as schematized in Fig. 7). Although a clear organization is difficult to observe at group-level, the single-subject analysis revealed a similar pattern as in the anterior lobe, where the eyes-to-toes gradients

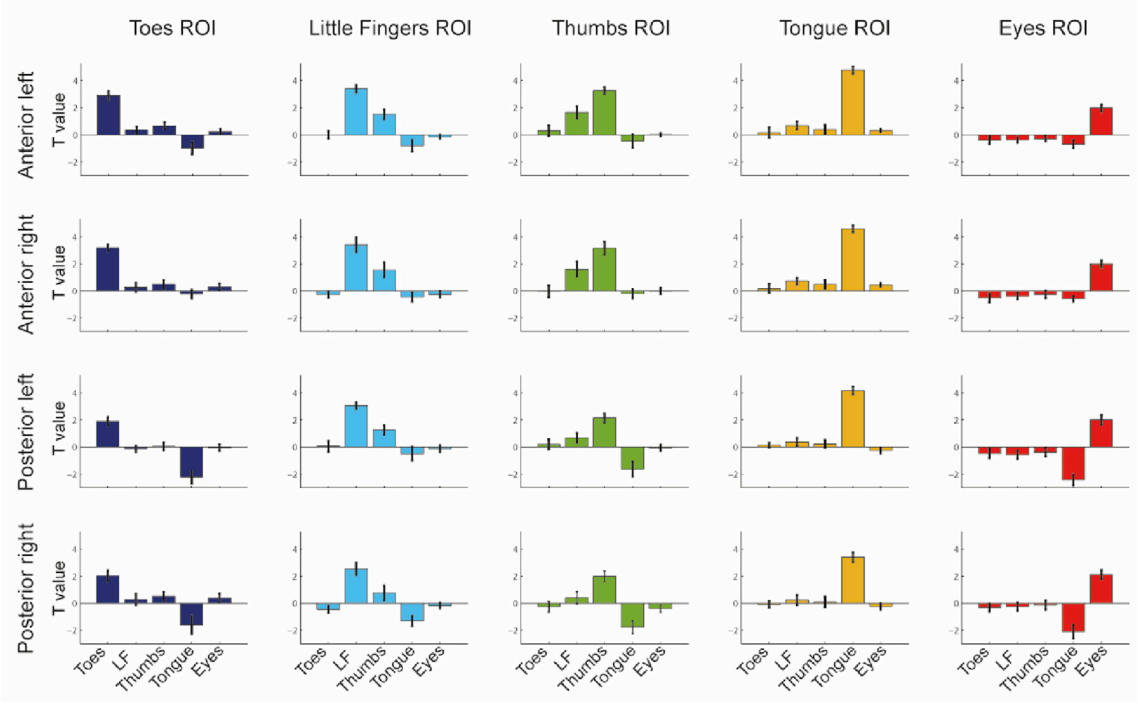

Fig. 3. T-values corresponding to different statistical contrasts testing for the five body parts extracted using the five labels as ROIs for the four cerebellar regions. The bar plots represent the mean across participants with the error bars representing the standard deviation.

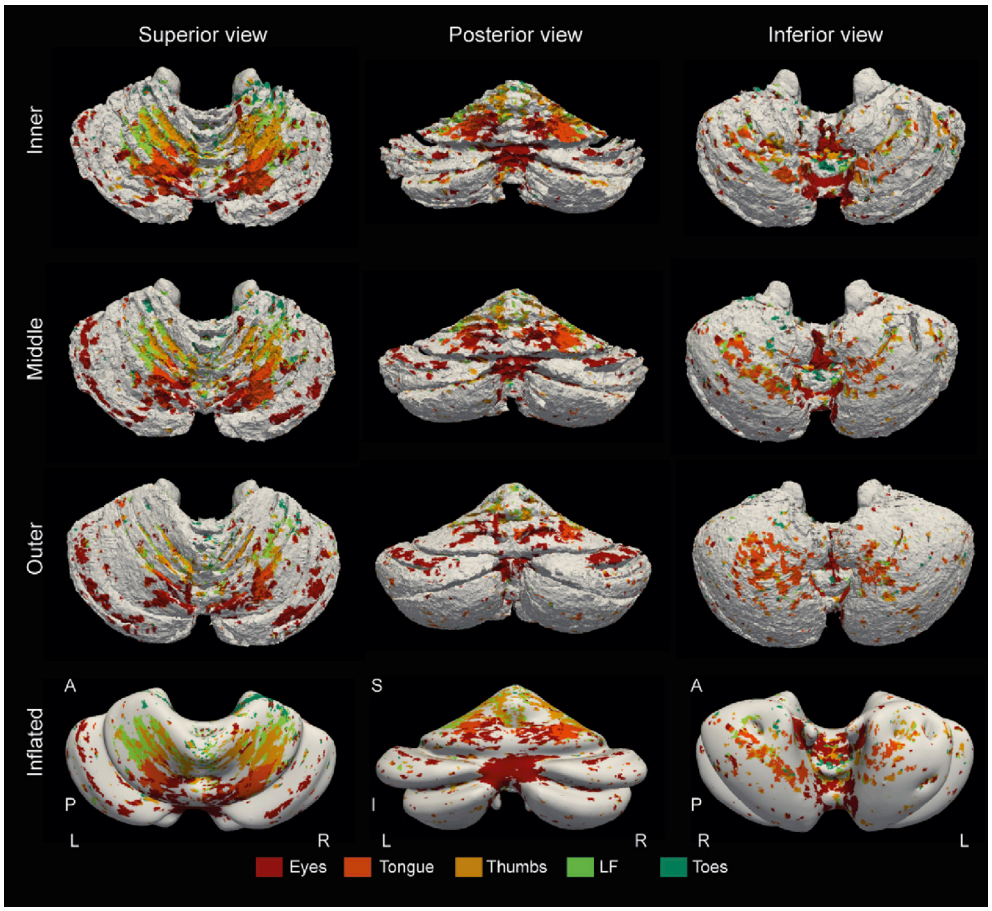

Fig. 4. Averaged inner, middle, outer and inflated cerebellar surfaces on which the label maps resulting from the second level analysis F-test (nonparametric test, CDT = 0.001, $p < .05$ FEW-corrected) used as a mask where each voxel was attributed to the body part showing the highest T-value are projected. The averaged surfaces are obtained from the average of subject-specific surfaces brought into the CHROMA space. The inflated surface is based on the surface of the CHROMA atlas. L/R stands for left/right orientations, A/P for anterior/posterior orientations and S/I for superior/inferior orientations.

are represented in a medio-posterior to latero-anterior fashion. The nature of this discrepancy is not clear. This might come from the cerebellar normalisation across participants or the large variability obtained at single-subject level (maximal number of overlaps equals 8 over 9 participants) yielding to group activity that does not pass the nonparametric test threshold. The posterior lobe has previously been characterized as showing more between-subject variability (van der Zwaag et al., 2013), with substantial differences in gradient orientations of digit representation, and even an absence of such a gradient in a group analysis (Wiestler et al., 2011). It is important to notice that although our results seem to indicate a higher variability in the posterior lobe, this could be due to differences in the segmentation and normalisation results. The somatotopic gradient seen here is much more consistent than predicted by earlier studies using an analysis in 3D (van der Zwaag et al., 2013; Wiestler et al., 2011). A full quantification of variability would require further improvements in the surface generation procedure as well as, most likely, a larger dataset. Testing for the arm, hand, lips and foot, Grodd et al. (2001) suggested that their representations could be somatotopically arranged although some parts were juxtaposed. Using functional connectivity, the presence of a foot-hand-tongue gradient (Buckner et al., 2011) was observed. However, as noted by the authors, this functional connectivity analysis only took into account the cerebral-cerebellar relationship and did not include information about the afferent and efferent pathways from the spinal cord as is the case with a motor task. A similar foot-hand-tongue pattern was also obtained with task activation maps from a very large Human Connectome Project dataset (n = 787; Guell et al., 2018a). Early investigations in monkey suggested that the posterior lobe somatotopic organization showed a bilateral embryo-shaped homunculus predominantly located in lobule VIIb (Snider and Eldred, 1951), which is also consistent with the results obtained by Grodd et al. (2001). In our case, the presence or absence of such embryo-shaped homunculus cannot be confirmed or disproved, as this would require inclusion of more central body parts such as the arms, legs or trunk. The difficulty in obtaining a robust somatotopic gradient in the posterior lobe is likely due to the challenges of imaging the cerebellum during both the acquisition and processing steps. For instance, the cerebellum is located in a region where the B_1 field is suboptimal when data are acquired with a traditional head coil and the posterior lobe is the cerebellar region the most effected by the lack of B_1 signal. In this study, dielectric pads were used to reduce this effect (Vaidya et al., 2018), however, the SNR obtained in the posterior lobe is still less than the SNR in the anterior lobe. Finally, the inter-body part distance is shorter in the cerebellum, especially in the posterior lobe (<20 mm), than what is observed in the cerebral cortex (Sanchez Panchuelo et al., 2018; Serino et al., 2017). This necessitates very high resolution functional acquisitions combined with structural data of sufficient quality to enable a precise single-subject level segmentation and mapping. The current study had sufficient resolution to resolve the five distal body representations targeted here, and profited from a surface reconstruction to visualise the results.

The most robust and largest body part representations were obtained for the tongue and fingers, which is consistent with their representation in motor and somatosensory cortices (Penfield and Boldrey, 1937). The tongue representation was bilaterally found in lobules VI, as already previously observed (Nitschke et al., 2007; Grodd et al., 2001), and between lobules VIIb and VIIIa (weak correlation in lobules VIII found in Grodd et al. (2001)). The somatotopic representation of the tongue shows overlaps with activity triggered by speech and song production (Callan et al., 2007).

As expected, the little finger and thumb representations were relatively close to each other as confirmed by the COG distances (6.2 and 6.8 mm for left and right hemispheres, respectively). The averaged distance

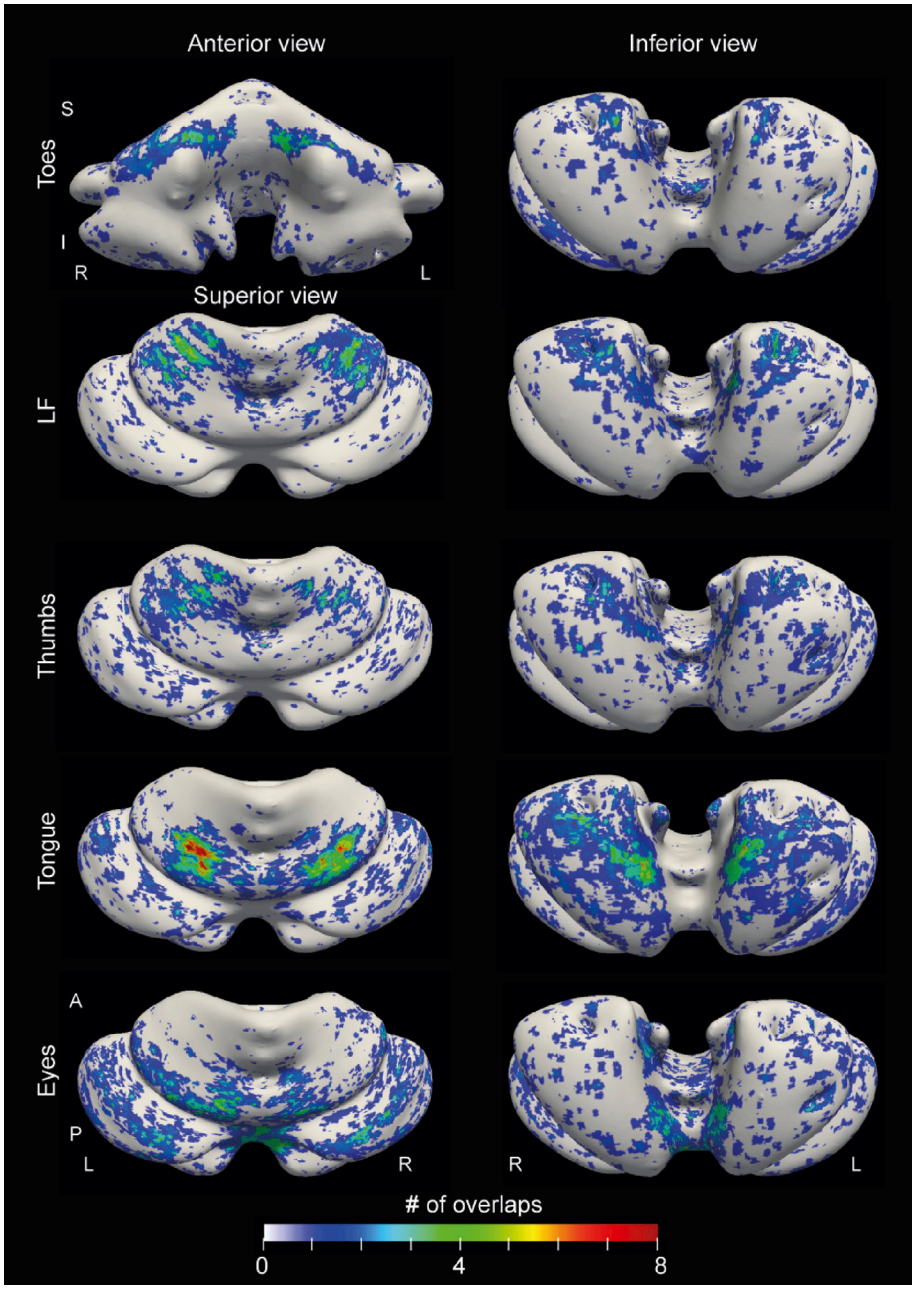

Fig. 5. Inflated surface of the CHROMA atlas on which the number of overlaps for each body parts is mapped. The overlap maps are generated from the addition of the respective binarized label maps. L/R stands for left/right orientations, A/P for anterior/posterior orientations and S/I for superior/inferior orientations.

between the five digits was shown to be small during both motor and tactile stimulations in lobule V (<3 mm and 3.7 mm, respectively; van der Zwaag et al., 2013; Wiestler et al., 2011).

A toe representation was found in lobule IV/VI and in lobule VIII. Toe-related activity has been found in lobules II-VI and also lobules VII-VIII (Rijntjes et al., 1999). Grodd et al. (2001) found similar foot areas with the main representation being in lobule IV followed by smaller clusters in lobules V and VI, but also in lobule IX, while Nitschke et al. (2007) found the foot being represented in lobules II-III. Although the comparison needs to be made with caution as our participants were asked to perform flexions of the toes and not of the feet (ankle), the overall foot representation seems to be the most anterior of the different body parts.

Beside the eye representations found as part of the anterior and posterior somatotopic gradients in lobules VI and VIIb-CrusII, additional activation was found in the vermis and Crus I. It was recently shown that the cerebellum contains retinotopic maps, which were mainly located in VIIIb and in the oculomotor vermis (van Es et al., 2018), corresponding well with the clusters found for simple eye movements here. Additionally, several studies have shown bilateral cerebellar activity related to visually guided eye saccades (Hayakawa et al., 2002; Stephan et al., 2002) in the cerebellar oculomotor vermis, which has been suggested to control the adaptation of saccades and smooth pursuits (Voogd et al., 2012), Crus I, Crus II, lobules VI and VIII. Finally, a pro-saccades/anti-saccades task showed activity in the oculomotor vermis, Crus I, Crus II, lobule VIIb and VIII (Batson et al., 2015). These previous results are in good agreement with the eye representations obtained in our study.

What the functional differences are between the two somatotopic representations in the cerebellum is still not clear. It has been proposed that the anterior lobe is linked to motor planning, while the posterior lobe would be more related to motor execution (Riecker et al., 2005). However, this conclusion seems to contrast with a recent study

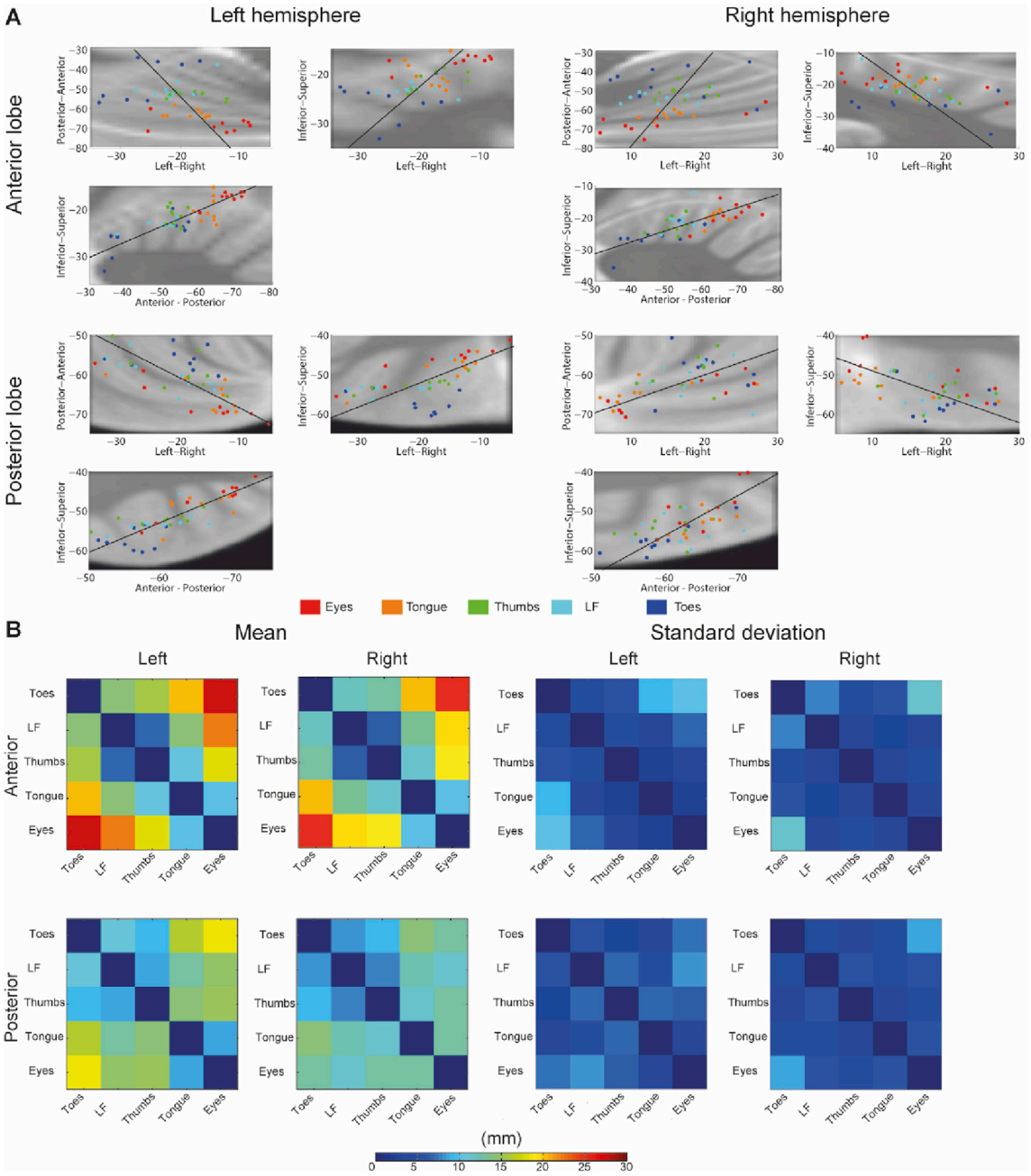

Fig. 6. A) Center of gravity (COG) maps for each participant and body part for the four cerebellar subdivisions overlaid on the CHROMA template: the left and right anterior lobes (including lobules I, II, III, IV, V and VI) and left and right posterior lobes (including lobules VIIb, VIIIa, VIIIb, IX and X). Each graph represents one of the three plans (axial, coronal and sagittal). The line represents the first principal component projected onto the corresponding plane. B) The Euclidean distances (in mm) between the COG for the four cerebellar subdivisions. Left graphs represent the mean across participants and right graphs represent the standard deviation.

suggesting that the representation of the posterior lobe corresponds to a less extreme level of information processing and requires a higher level of task focus (Guell et al., 2018c). Moreover, a functional connectivity study found that the anterior lobe was connected to primary and supplementary motor cortices, while lobule VIII was connected to adjacent regions having more integrative functions (Kipping et al., 2013). This alternative hypothesis is consistent with the results obtained in patients suffering from cerebellar strokes who showed motor impairment with lesions affecting the anterior lobe, while no significant motor impairment was observed with lesions in lobule VIII (Stoodley et al., 2016). In the present study, the simple motor task did not enable us to behaviourally separate the two regions.

Taking into account the different functional mapping studies of the cerebellum, it is clear that a lobule-wise parcellation of the cerebellum is not functionally meaningful as specific functions span across several lobules. However, it has been shown that the cerebellum can be parcellated according to different physiological and anatomical patterns such as the longitudinal zones defined by the inputs from the inferior olive and the corticonuclear outputs or the parasagittal stripes corresponding to the expression levels of specific genes, i.e. zebrin II gene, both of these patterns being to a certain degree co-localized (Apps and Hawkes, 2009). In a first attempt to highlight the microstructural variations of the cerebellum by using T_1 and T_2* quantitative mapping, we were able to show medio-lateral variations of these MR values, having a similar orientation to the longitudinal zones (Boillat et al., 2018). However, the exact direction of this pattern does not seem to match the somatotopic gradients

Table 1
Results of the Page test testing the hypothesis of an ordering of the different body parts based on the coordinates along the first PC. It tests the hypothesis that the gradient is organized in the following order (eyes – tongue – thumbs – little fingers – toes). The test provided an L-statistic, which is the equivalent of an F value for an F-test. Values for statistical significance are obtained from Page (1963). A p-value smaller than 0.05 means that the different body parts are organized in an ordered manner. The averaged statistical results of 1000 random permutations are also showed.

	Somatotopic pattern		Random permutation	
	L statistic	p-value	L statistic	p-value
Anterior left	488	.001	404	.95
Anterior right	474	.001	405	1
Posterior left	461	.001	405	1
Posterior right	444	.01	406	.95

observed in the current study, which is consistent with a recent study showing no spatial correlation between the cerebellar functional organization and microstructural changes as measured by the T_1w/T_2w ratio (Guell et al., 2018b). A study in mice suggested that the different parasagittal stripes exhibit within-stripe synchronization, but increase the within- and between-stripe synchronizations during sensory stimulation (Tsutsumi et al., 2015). Therefore, the (micro)structure-function relationship of the cerebellum remains an open area of research which can substantially benefit from high-resolution fMRI acquisitions. Although we were able to show a consistent somatotopic organization across both the anterior and posterior lobes of the cerebellum with a fine level of details, some parameters should be taken into consideration. As the visualisation of such patterns, especially in the posterior lobe, strongly depends on the B_1 field, data acquired with a dedicated surface coil covering the upper neck area would probably yield higher SNR providing lower variability in the mapping of the posterior lobe. The use of bilateral movements compared to unilateral movements might also provide slightly different somatotopic maps as unilateral movements have been shown to activate also partially the contralateral cerebellar hemisphere (Schlerf et al., 2010). Slightly different maps might also be obtained in case of a self-paced paradigm that may engage a distinct set of regions (Witt et al., 2008). Additionally, the task used in the current study involved both motor and sensory functions, which may not be exactly colocalized (Wiestler et al., 2011) and result in "diluted" maps. In case of the finger movements, especially for the little fingers, residual movements from adjacent fingers might also be present that could lead to a less precise representation. Given the low crosstalk (Fig. 3), this effect is deemed to be small. Another limitation of this study is the lack of movement monitoring. Although the participants were asked to follow a paced cue, their performance was not assessed, which could potentially form a source of between-subject variability. In addition, it has been shown using electrophysiology in rats that the body is represented in a fractured manner, where each body part representation is broken up into smaller, entangled representations at sub-milometer scales (Shambes et al., 1978). Such fractured representations, although maybe of a different nature, were also observed in the human motor cortex (Graziano and Aflalo, 2007; Meier et al., 2008). In the present study, the high-resolution acquisition revealed multiple representations of each body part in a single region (i.e. left anterior lobe), especially at single-subject level. As the size of the fractured somatotopy "patches" is still not known in the human cerebellum, further investigations would be required to determine whether these fractured representations are actual body part representation and not due to noise. The potential presence of a fractured somatotopy might render our COG approach not optimal as several clusters per lobe per hemisphere for each body part would have to be considered instead of one in the present study. Finally, even though our results showed small amounts of overlap across body parts, to which degree the cerebellar somatotopic organization can be modelled as segregated body part representations is not clear. In the motor cortex, several overlapping topographic organizations such as overlapping and segregated somatotopic maps of the body, a map of hand location in space and a map of movements were observed, especially in the monkey (Aflalo and Graziano, 2006; Graziano and Aflalo, 2007). Whether, such more complex topographic representations are present in the cerebellum

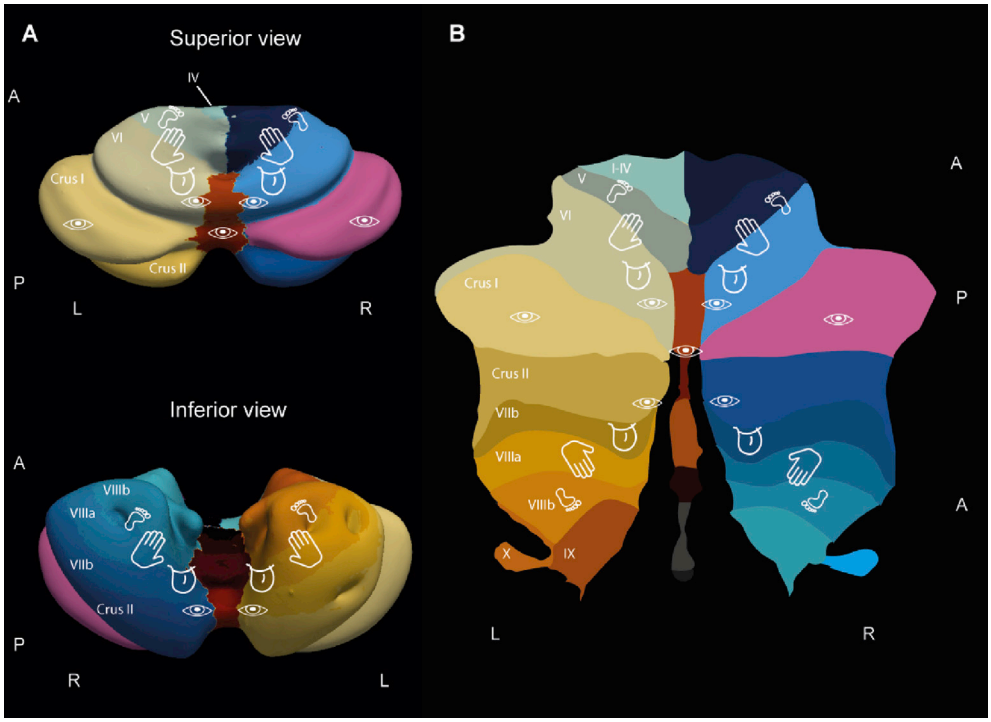

Fig. 7. A) Schematic representation of the somatotopic organization obtained in the current study showed on the inflated surface on which the CHROMA lobule atlas is mapped. The location and relative size of the different symbols summarize the results of the group- and subject-level analysis. B) Similar representation on a flatmap from the SUIT toolbox (Diedrichsen and Zotow, 2015).

is not clear, but some results might point in this direction. For instance, Mottolese et al. (2013) electrically stimulated the posterior cerebellum of human patients showing a rather intermingled somatotopic organization and areas that would activate multiple joints.

With this study, we were able to precisely define somatotopic maps in both anterior and posterior lobes of the cerebellum for five distal body parts. We demonstrated that both bilateral anterior and posterior lobes contain somatotopic gradients organized in a medio-posterior to latero-anterior fashion where the eyes, tongue, thumbs, little fingers and toes are represented. This study also shows the necessity of having sufficient B_1 field for the data acquisition and the need for subject-level analysis compared to the more traditional group-level analysis, especially for the posterior lobe.

Data and code availability

The custom Matlab and CBS Tools code can be found at https://github.com/yboillat/Cerebellum_somatotopy. The single-subject T maps in native space can be found at https://identifiers.org/neurovault.image:317112.

Declaration of competing interest

The authors have no conflicts of interest to disclose.

CRediT authorship contribution statement

Yohan Boillat: Conceptualization, Methodology, Data curation, Formal analysis, Writing - original draft. **Pierre-Louis Bazin:** Methodology, Writing - review & editing. **Wietske van der Zwaag:** Conceptualization, Methodology, Writing - review & editing, Funding acquisition, Supervision.

Acknowledgments

This work was supported by the Centre d'Imagerie BioMédicale (CIBM) of the UNIL, UNIGE, HUG, CHUV, and EPFL and the Leenaards and Jeantet Foundations and the Swiss National Science Foundation Grant #31003A_149983 and #31003A_153070.

Appendix A. Supplementary data

Supplementary data to this article can be found online at https://doi.org/10.1016/j.neuroimage.2020.116624.

References

Adrian, E.D., 1943. Afferent areas in the cerebellum connected with the limbs. Brain 66, 289–315. https://doi.org/10.1093/brain/66.4.289.

Aflalo, T.N., Graziano, M.S. a, 2006. Possible origins of the complex topographic organization of motor cortex: reduction of a multidimensional space onto a two-dimensional array. J. Neurosci. 26, 6288–6297. https://doi.org/10.1523/JNEUROSCI.0768-06.2006.

Akselrod, M., Martuzzi, R., Serino, A., van der Zwaag, W., Gassert, R., Blanke, O., 2017. Anatomical and functional properties of the foot and leg representation in areas 3b, 1 and 2 of primary somatosensory cortex in humans: a 7T fMRI study. Neuroimage 159, 473–487. https://doi.org/10.1016/j.neuroimage.2017.06.021.

Apps, R., Hawkes, R., 2009. Cerebellar cortical organization: a one-map hypothesis. Nat. Rev. Neurosci. 10, 670–681. https://doi.org/10.1038/nrn2698.

Avants, B.B., Epstein, C.L., Grossman, M., Gee, J.C., 2008. Symmetric diffeomorphic image registration with cross-correlation: evaluating automated labeling of elderly and neurodegenerative brain. Med. Image Anal. 12, 26–41. https://doi.org/10.1016/j.media.2007.06.004.

Batson, M.a., Petridou, N., Klomp, D.W.J., Frens, M.a., Neggers, S.F.W., 2015. Single session imaging of cerebellum at 7 Tesla: obtaining structure and function of multiple motor subsystems in individual subjects. PloS One 10, e0134933. https://doi.org/10.1371/journal.pone.0134933.

Bazin, P.L., Weiss, M., Dinse, J., Schäfer, A., Trampel, R., Turner, R., 2013. A computational framework for ultra-high resolution cortical segmentation at 7 Tesla. Neuroimage 93, 201–209. https://doi.org/10.1016/j.neuroimage.2013.03.077.

Bazin, P.L., Weiss, M., Dinse, J., Schäfer, A., Trampel, R., Turner, R., 2014. A computational framework for ultra-high resolution cortical segmentation at 7 Tesla. Neuroimage 93, 201–209. https://doi.org/10.1016/j.neuroimage.2013.03.077.

Bogovic, J.a., Prince, J.L., Bazin, P.-L., 2013. A multiple object geometric deformable model for image segmentation. Comput. Vis. Image Understand. 117, 145–157. https://doi.org/10.1016/j.cviu.2012.10.006.

Boillat, Y., Bazin, P.-L., O'Brien, K., Fartaria, M.J., Bonnier, G., Krueger, G., Van der Zwaag, W., Granziera, C., 2018. Surface-based characteristics of the cerebellar cortex visualized with ultra-high field MRI. Neuroimage 172, 1–8. https://doi.org/10.1016/j.neuroimage.2018.01.016.

Buckner, R.L., Krienen, F.M., Castellanos, a., Diaz, J.C., Yeo, B.T.T., 2011. The organization of the human cerebellum estimated by intrinsic functional connectivity. J. Neurophysiol. 106, 2322–2345. https://doi.org/10.1152/jn.00339.2011.

Callan, D.E., Kawato, M., Parsons, L., Turner, R., 2007. Speech and song: the role of the cerebellum. Cerebellum 6, 321–327. https://doi.org/10.1080/14734220601187733.

Diedrichsen, J., Zotow, E., 2015. Surface-based display of volume-averaged cerebellar imaging data. PloS One 10, 1–18. https://doi.org/10.1371/journal.pone.0133402.

Eggenschwiler, F., Kober, T., Magill, A.W., Gruetter, R., Marques, J.P., 2012. SA2RAGE: a new sequence for fast B1+ -mapping. Magn. Reson. Med. 67, 1609–1619. https://doi.org/10.1002/mrm.23145.

Gallichan, D., Marques, J.P., Gruetter, R., 2015. Retrospective correction of involuntary microscopic head movement using highly accelerated fat image navigators (3D FatNavs) at 7T. Magn. Reson. Med. 1039, 1030–1039. https://doi.org/10.1002/mrm.25670.

Glover, G.H., Li, T.Q., Ress, D., 2000. Image-based method for retrospective correction of physiological motion effects in fMRI: RETROICOR. Magn. Reson. Med. 44, 162–167. https://doi.org/10.1002/1522-2594(200007)44:1<162::AID-MRM23>3.0.CO;2-E.

Graziano, M.S.A., Aflalo, T.N., 2007. Mapping behavioral repertoire onto the cortex. Neuron 56, 239–251. https://doi.org/10.1016/j.neuron.2007.09.013.

Grodd, W., Hülsmann, E., Lotze, M., Wildgruber, D., Erb, M., 2001. Sensorimotor mapping of the human cerebellum: fMRI evidence of somatotopic organization. Hum. Brain Mapp. 13, 55–73. https://doi.org/10.1002/hbm.1025.

Guell, X., Gabrieli, J.D.E., Schmahmann, J.D., 2018a. Triple representation of language, working memory, social and emotion processing in the cerebellum: convergent evidence from task and seed-based resting-state fMRI analyses in a single large cohort. Neuroimage 172, 437–449. https://doi.org/10.1016/j.neuroimage.2018.01.082.

Guell, X., Schmahmann, J.D., Gabrieli, J.D.E., 2018b. Functional specialization is independent of microstructural variation in cerebellum but not in cerebral cortex. bioRxiv, 424176. https://doi.org/10.1101/424176.

Guell, X., Schmahmann, J.D., Gabrieli, J.D.E., Ghosh, S.S., 2018c. Functional gradients of the cerebellum. eLife 7, 1–22. https://doi.org/10.7554/elife.36652.

Han, X., Pham, D.L., Tosun, D., Rettmann, M.E., Xu, C., Prince, J.L., 2004. CRUISE: cortical reconstruction using implicit surface evolution. Neuroimage 23, 997–1012. https://doi.org/10.1016/j.neuroimage.2004.06.043.

Hayakawa, Y., Nakajima, T., Takagi, M., Fukuhara, N., Abe, H., 2002. Human cerebellar activation in relation to saccadic eye movements: a functional magnetic resonance imaging study. Ophthalmologica 216, 399–405. https://doi.org/10.1159/000067551.

Jenkinson, M., Smith, S., 2001. A global optimisation method for robust affine registration of brain images. Med. Image Anal. 5, 143–156. https://doi.org/10.1016/S1361-8415(01)00036-6.

Kipping, J.a., Grodd, W., Kumar, V., Taubert, M., Villringer, A., Margulies, D.S., 2013. Overlapping and parallel cerebello-cerebral networks contributing to sensorimotor control: an intrinsic functional connectivity study. Neuroimage 83, 837–848. https://doi.org/10.1016/j.neuroimage.2013.07.027.

Marques, J.P., Gruetter, R., 2013. New developments and applications of the MP2RAGE sequence–focusing the contrast and high spatial resolution R1 mapping. PloS One 8, e69294. https://doi.org/10.1371/journal.pone.0069294.

Marques, J.P., Gruetter, R., Van Der Zwaag, W., 2012. In vivo structural imaging of the cerebellum, the contribution of ultra-high fields. Cerebellum 11, 384–391. https://doi.org/10.1007/s12311-010-0189-2.

Marques, J.P., Kober, T., Krueger, G., van der Zwaag, W., Van de Moortele, P.-F., Gruetter, R., 2010a. MP2RAGE, a self bias-field corrected sequence for improved segmentation and T1-mapping at high field. Neuroimage 49, 1271–1281. https://doi.org/10.1016/j.neuroimage.2009.10.002.

Marques, J.P., van der Zwaag, W., Granziera, C., Krueger, G., Gruetter, R., 2010b. Cerebellar cortical layers: in vivo visualization with structural high-field-strength MR imaging. Radiology 254, 942–948. https://doi.org/10.1148/radiol.09091136.

Martuzzi, R., van der Zwaag, W., Farthouat, J., Gruetter, R., Blanke, O., 2014. Human finger somatotopy in areas 3b, 1, and 2: a 7T fMRI study using a natural stimulus. Hum. Brain Mapp. 35, 213–226. https://doi.org/10.1002/hbm.22172.

Meier, J.D., Aflalo, T.N., Kastner, S., Graziano, M.S.A., 2008. Complex organization of human primary motor cortex: a high-resolution fMRI study. J. Neurophysiol. 100, 1800–1812. https://doi.org/10.1152/jn.90531.2008.

Mottolese, C., Richard, N., Harquel, S., Szathmari, A., Sirigu, A., Desmurget, M., 2013. Mapping motor representations in the human cerebellum. Brain 136, 330–342. https://doi.org/10.1093/brain/aws186.

Nitschke, F.M., Kleinschmidt, A., Wessel, K., Frahm, J., 2007. Somatotopic motor representation in the human anterior cerebellum. Brain 119, 1023–1029. https://doi.org/10.1093/brain/119.3.1023.

Page, E.B., 1963. Ordered hypotheses for multiple treatments: a significance test for linear ranks. J. Am. Stat. Assoc. 58, 216–230. https://doi.org/10.1080/01621459.1963.10500843.

Penfield, W., Boldrey, E., 1937. Somatic motor and sensory representation IN the cerebral cortex of man as studied BY electrical stimulation. Brain 60, 389–443. https://doi.org/10.1093/brain/60.4.389.
Pham, D.L., 2001. Robust Fuzzy segmentation of magnetic resonance images. IEEE Symp. Comput. Med. Syst. 127–131.
Riecker, A., Mathiak, K., Wildgruber, D., Erb, M., Hertrich, I., Grodd, W., Ackermann, H., 2005. fMRI reveals two distinct cerebral networks subserving speech motor control. Neurology 64, 700–706. https://doi.org/10.1212/01.WNL.0000152156.90779.89.
Rijntjes, M., Buechel, C., Kiebel, S., Weiller, C., 1999. Multiple somatotopic representations in the human cerebellum. Neuroreport 10, 3653–3658. https://doi.org/10.1097/00001756-199911260-00035.
Sanchez Panchuelo, R.M., Besle, J., Schluppeck, D., Humberstone, M., Francis, S., 2018. Somatotopy in the human somatosensory system. Front. Hum. Neurosci. 12, 1–14. https://doi.org/10.3389/fnhum.2018.00235.
Schlerf, J.E., Verstynen, T.D., Ivry, R.B., Spencer, R.M.C., 2010. Evidence of a novel somatopic map in the human neocerebellum during complex actions. J. Neurophysiol. 103, 3330–3336. https://doi.org/10.1152/jn.01117.2009.
Serino, A., Akselrod, M., Salomon, R., Martuzzi, R., Blefari, M.L., Canzoneri, E., Rognini, G., Van Der Zwaag, W., Iakova, M., Luthi, F., Amoresano, A., Kuiken, T., Blanke, O., 2017. Upper limb cortical maps in amputees with targeted muscle and sensory reinnervation. Brain 140, 2993–3011. https://doi.org/10.1093/brain/awx242.
Shambes, G.M., Gibson, J.M., Welker, W., 1978. Fractured somatotopy in granule cell tactile areas of rat cerebellar hemispheres revealed by micromapping; pp. 94–105. Brain Behav. Evol. 15, 94–105. https://doi.org/10.1159/000123774.
Smith, S.M., 2002. Fast robust automated brain extraction. Hum. Brain Mapp. 17, 143–155. https://doi.org/10.1002/hbm.10062.
Snider, R.S., Eldred, E., 1951. Cerebro-cerebellar relationships in the monkey. J. Neurophysiol. 27–40, 1948.
Snider, R.S., Stowell, A., 1944. Receiving areas of the tactile, auditory, and visual systems in the cerebellum. J. Neurophysiol. 7, 331–357. https://doi.org/10.1152/jn.1944.7.6.331.
Stephan, T., Mascolo, A., Yousry, T.A., Bense, S., Brandt, T., Dieterich, M., 2002. Changes in cerebellar activation pattern during two successive sequences of saccades. Hum. Brain Mapp. 16, 63–70. https://doi.org/10.1002/hbm.10028.
Stoodley, C.J., MacMore, J.P., Makris, N., Sherman, J.C., Schmahmann, J.D., 2016. Location of lesion determines motor vs. cognitive consequences in patients with cerebellar stroke. Neuroimage Clin. 12, 765–775. https://doi.org/10.1016/j.nicl.2016.10.013.
Teeuwisse, W.M., Brink, W.M., Webb, A.G., 2012. Quantitative assessment of the effects of high-permittivity pads in 7 Tesla MRI of the brain. Magn. Reson. Med. 67, 1285–1293. https://doi.org/10.1002/mrm.23108.
Tsutsumi, S., Yamazaki, M., Miyazaki, T., Watanabe, M., Sakimura, K., Kano, M., Kitamura, K., 2015. Structure-function relationships between aldolase C/zebrin II expression and complex spike synchrony in the cerebellum. J. Neurosci. 35, 843–852. https://doi.org/10.1523/JNEUROSCI.2170-14.2015.
Vaidya, M.V., Lazar, M., Deniz, C.M., Haemer, G.G., Chen, G., Bruno, M., Sodickson, D.K., Lattanzi, R., Collins, C.M., 2018. Improved detection of fMRI activation in the cerebellum at 7T with dielectric pads extending the imaging region of a commercial head coil. J. Magn. Reson. Imag. 1–10. https://doi.org/10.1002/jmri.25936.
van der Zwaag, W., Jorge, J., Butticaz, D., Gruetter, R., 2015a. Physiological noise in human cerebellar fMRI. Magn. Reson. Mater. Phys. Biol. Med. 28, 485–492. https://doi.org/10.1007/s10334-015-0483-6.
van der Zwaag, W., Kusters, R., Magill, A., Gruetter, R., Martuzzi, R., Blanke, O., Marques, J.P., 2013. Digit somatotopy in the human cerebellum: a 7T fMRI study. Neuroimage 67, 1–9. https://doi.org/10.1016/j.neuroimage.2012.11.041.
van Es, D.M., van der Zwaag, W., Knapen, T., 2018. Retinotopic Maps of Visual Space in the Human Cerebellum bioRxiv 455170.
Voogd, J., Schraa-Tam, C.K.L., Van Der Geest, J.N., De Zeeuw, C.I., 2012. Visuomotor cerebellum in human and nonhuman primates. Cerebellum 11, 392–410. https://doi.org/10.1007/s12311-010-0204-7.
Waehnert, M.D., Dinse, J., Weiss, M., Streicher, M.N., Waehnert, P., Geyer, S., Turner, R., Bazin, P.L., 2014. Anatomically motivated modeling of cortical laminae. Neuroimage 93, 210–220. https://doi.org/10.1016/j.neuroimage.2013.03.078.
Wiestler, T., McGonigle, D.J., Diedrichsen, J., 2011a. Integration of sensory and motor representations of single fingers in the human cerebellum. J. Neurophysiol. 105, 3042–3053. https://doi.org/10.1152/jn.00106.2011.
Witt, S.T., Laird, A.R., Meyerand, M.E., 2008. Functional neuroimaging correlates of finger-tapping task variations: an ALE meta-analysis. Neuroimage 42, 343–356. https://doi.org/10.1016/j.neuroimage.2008.04.025.